Gold nanocrystals in high-temperature superconducting films: creation of pinning patterns of choice

New Journal of Physics
The open access journal for physics

Gold nanocrystals in high-temperature superconducting films: creation of pinning patterns of choice

C Katzer[1,4], C Stahl[2], P Michalowski[1], S Treiber[2], F Schmidl[1], P Seidel[1], J Albrecht[3] and G Schütz[2]

[1] Institute of Solid State Physics, Friedrich-Schiller University Jena Helmholtzweg 5, D-07743 Jena, Germany
[2] Max-Planck-Institute for Intelligent Systems Heisenbergstrasse 3, D-70569 Stuttgart, Germany
[3] Aalen University Beethovenstrasse 1, D-73430 Aalen, Germany
E-mail: christian.katzer@uni-jena.de

New Journal of Physics **15** (2013) 113029 (12pp)
Received 2 April 2013
Published 13 November 2013
Online at http://www.njp.org/
doi:10.1088/1367-2630/15/11/113029

Abstract. One of the major drawbacks for applications of high-temperature superconducting films is that magnetic flux is not completely expelled but penetrates the film in the form of flux vortices. Any motion of these vortices is accompanied by magnetic noise and prevents larger supercurrents. Thus, an effective pinning of flux vortices is a prerequisite for applications based on thin films of high-temperature superconductors such as coated conductors or magnetic sensor devices. However, particular superconducting structures such as tunnel barriers or flux guides suffer from increased pinning forces. We report that adding thin gold layers to the production process of epitaxial films of the high-temperature superconductor $YBa_2Cu_3O_{7-\delta}$ allows the fabrication of superconducting films with spatially varying flux pinning properties. This paves the way for an easy realization of custom tailored current carrying capabilities in arbitrary patterns. Critical current densities of already strong pinning films can be locally enhanced up to 150% to prepare a material of choice at a position of choice for the realization of high-quality electronic devices with improved performance.

[4] Author to whom any correspondence should be addressed.

Contents

1. Introduction

The concept of an artificially increased pinning landscape in thin films of high-temperature (High-T_c) superconductors is highly attractive for many applications. Often the most crucial property for reasonable operation of superconducting films is the efficient suppression of flux line motion to avoid unwanted dissipation and magnetic noise. However, using high-temperature superconductors in more complex electronic applications such as magnetic sensor devices or logic elements for quantum computing usually requires an implementation of Josephson junctions or weak links [1, 2]. For a properly working Josephson junction, however, the values of the critical current I_c must not be too high [3, 4]. In this case an increase of the critical current density by artificial pinning centres (APCs) is non-desirable. These border conditions directly require a technique of spatially resolved custom tailoring of the flux pinning landscape if a significant improvement of the properties of such devices is to be addressed.

If one cannot avoid vortex penetration into the superconductor in the first place [5], one can suppress vortex motion through pinning the flux lines at inherent or artificial pinning centres. Several efficient techniques are currently known to introduce such artificial pinning centres into thin films of optimally doped high-temperature superconducting $YBa_2Cu_3O_{7-\delta}$ (YBCO) [6–20].

A very effective way to enhance the vortex pinning performance is the inclusion of barium zirconate (BZO) nanoparticles which can substantially increase the critical current density in a wide region of temperatures and magnetic fields [21–24]. Recently it has been shown that the origin of this effect is local strain formation creating an additional isotropic pinning force density [25]. However, the existing BZO technology only allows a complete, area-wide modification of superconducting films. Although it could be shown that a sophisticated treatment of YBCO films by heavy-ion irradiation can generate artificial structures of controlled critical current density distributions [26], this method unfortunately only allows shifting critical currents towards lower values. More promising results could be achieved by prepatterning the substrates. Here, an ion implantation into the substrate before film growth can lead to films with modified microstructure, exhibiting slightly enhanced critical current density values. However, although the experimental effort is enormous, the achieved current increase is rather limited [27–29]. In this paper we show that it is possible to use a dewetting process of thin gold layers for the controlled inclusion of gold nanoparticles into thin epitaxial YBCO films. This can in particular be done under geometric constraints on a (sub-) micrometre scale. A spatially resolved modification of the superconducting film can tailor local pinning

properties to control the local motion of magnetic vortices and thus the local critical current density. Being able to control local properties allows one to take care of different functional requirements in different areas of an individual superconducting film. This means, for example, a thin film superconducting quantum interference device (SQUID) gradiometer structure can be manufactured where strong pinning in the antenna structures can be combined with grain boundary Josephson junctions with lower critical currents. The combination of both engineering steps would lead to a significant increase in the signal to noise ratio of the device [20].

2. Results and discussion

2.1. Sample preparation and patterning

Laser-assisted deposition techniques like pulsed laser deposition (PLD) offer the possibility of growing epitaxial thin films of a high crystalline quality whilst ensuring the right film stoichiometry. Furthermore, PLD allows growing thin films in an oxygen atmosphere, thus being suitable to fabricate YBCO thin films with optimized oxygen context. Here we will consider YBCO as the superconducting material of choice because of its low anisotropy compared to other high-T_c materials [30]. Prior to the YBCO deposition we coated our polished $SrTiO_3$ (100) single crystal substrates with a thin gold layer ($t_{Au} \approx 3$ nm), also using PLD in a vacuum ($p_0 < 4 \times 10^{-4}$ Pa). The coated substrates were then heated to 780 °C, which was found to be the best temperature to grow YBCO films exhibiting good superconducting properties such as high critical temperature and critical current density, together with a high crystalline quality. To guarantee the optimum oxygen stoichiometry the deposition of 50 nm YBCO was carried out in an oxygen atmosphere of $p_{O2} = 50$ Pa. Using a KrF excimer laser operating at a wavelength of 248 nm and a pulse duration of 25 ns the deposition rate was found to be 20 nm min^{-1} at a laser fluence of 2.2 J cm^{-2}. The laser repetition rate was set to 5 Hz. Subsequently, the resulting thin films were cooled to room temperature using a cooling rate of 50 K min^{-1} in an oxygen atmosphere of 80 kPa to induce the orthorhombic phase.

Due to the high temperatures during YBCO thin film deposition one can observe a dewetting of the Au layer and the formation of crystalline Au nanoparticles within the growing YBCO matrix. In this way the growth conditions of the YBCO thin film are modified [31]. Owing to their distribution over the whole YBCO layer the Au nanocrystals create inhomogeneous strain at the nanoscale which efficiently creates an additional pinning force density and thus increases the YBCO critical current density [25]. At the same time this reduces the flux noise of superconducting devices as we reported elsewhere [20]. Furthermore, the Au nanoparticles also affect the behaviour of grain boundary junctions i.e. decreasing the junctions' critical current density as we could show elsewhere [32]. However, this might be unwanted in those antenna regions of planar galvanically coupled SQUID gradiometers [33] which are crossed by the grain boundary due to a reduced carrying capability of screening currents. Hence, one needs a patterning of the Au seed layer to restrict the Au nanoparticles to well-defined areas.

The patterning of the gold film can be easily achieved by a lithographic process. In our experiments this was done using photolithography. The cleaned substrates were coated with the photoresist AZ5214E from Microchemicals GmbH (Ulm, Germany) using spin coating. The photoresist was patterned using a photomask and a Quintel q-2001c mask aligner. The structure

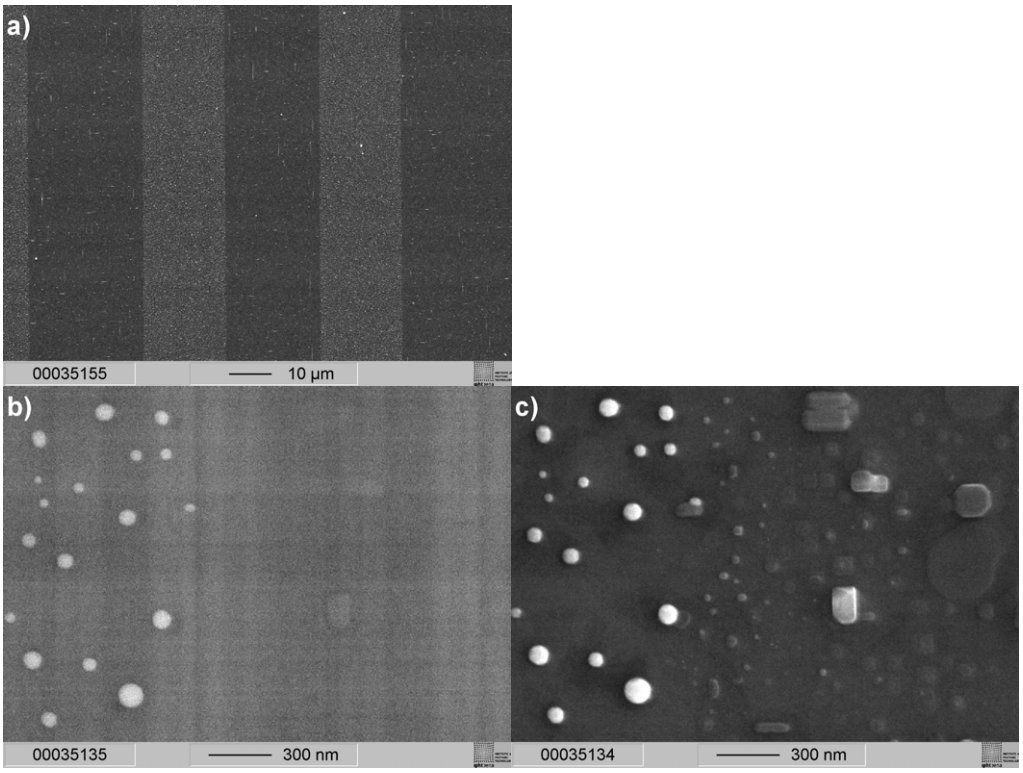

Figure 1. SEM micrograph of the surface of a thin film of YBCO grown on a partly Au covered substrate. The Au seed layer was patterned into small stripes to restrict the Au nanoparticles to only well separated areas. (a) Vertically oriented stripes are seen, identifying those parts containing gold (brighter areas). (b) Backscattered electron image of the border line between two stripes in a higher magnification. The circular white structures on the left side are the gold nanoparticles, which can easily be identified using material contrast. Note that the border line appears to be sub-micron sharp. (c) Secondary electron image of the same area. Interestingly, outgrowths of secondary YBCO phases can only be found in the areas containing no Au particles (right side of panel c).

then was developed in 726MIF (Microchemicals). After the subsequent deposition of the Au seed layer the remaining photoresist was stripped of using acetone. The acetone was removed by rinsing with isopropyl alcohol and the patterned Au layer was overgrown by YBCO as stated above.

2.2. SEM and white-light interferometry results

Figure 1 depicts a micrograph of the surface of the YBCO film in two different magnifications obtained by scanning electron microscopy. In panel (a) a vertically oriented stripe-like structure can be seen. The brighter stripes refer to parts where Au is incorporated into the YBCO film. In this case 20 μm wide structures had been prepared. Panel (b) depicts an area at the borderline of two stripes with a higher magnification. White, circular-shaped structures which represent the incorporated Au nanoparticles are visible. We find that the distribution of these nanoparticles

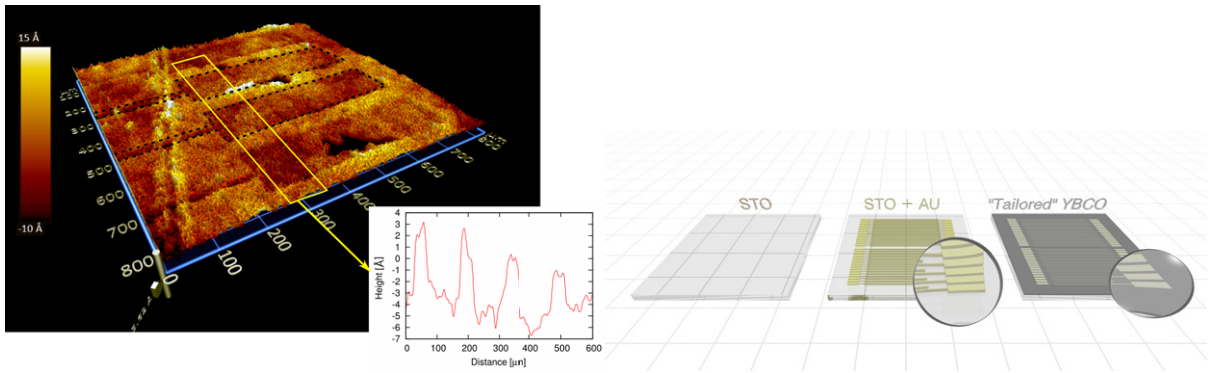

Figure 2. Left: three-dimensional representation of the surface topography obtained by white-light interferometry. Right: sketch allowing an identification of those thin film parts where Au nanoparticles were embedded. Interestingly, these areas appear to be 0.6 nm thinner than the pristine areas. Note that a sharp border line between the two different areas is found which is in good agreement with the SEM images.

is limited to the left part of the image which can easily be seen due to the material specific contrast of backscattered electrons in this image. It is important to note that a (sub-micrometre) sharp borderline is found which separates the two regions. These sharp boundaries between both areas are typical and we did not note any lateral diffusion of Au particles to areas of non-modified YBCO. Thus, the only limitations of micro structuring our samples with Au particles were set by our lithographic process. Panel (c) depicts the same area as panel (b) but utilizing the topographic contrast of secondary electron imaging. It is noteworthy that some outgrowth of secondary phases can be found in those areas containing no Au particles, which is typical for YBCO thin films (see the right side of panel (c)). Interestingly, it seems that the distribution density of those precipitates can be reduced by incorporating Au particles, since fewer precipitates can be found in areas containing gold. This could be due to a relaxation of macroscopic strains within the film at the Au particles. This would prevent the formation of defects such as dislocations which are known to contribute to the formation of precipitates in YBCO thin films [34]. The fact that the distribution density of precipitates is reduced in the Au modified areas leads to the conclusion that an enhanced pinning of flux vortices is not caused by additional outgrowths and extended defects but by the additional inhomogeneous strain at the nanoscale, creating an additional pinning force density induced by Au nanoparticles [25].

Figure 2 (left) depicts a three-dimensional representation of the surface topography which has been obtained by white-light interferometry. The section displays an area of $800 \times 800\ \mu m^2$ of a partly modified YBCO film. The sketch nearby (figure 2 right) allows an easy identification of the thin film parts where gold nanoparticles are embedded. A quantitative analysis leads to the fact that the areas with Au particles are about 0.6 nm thinner than the areas without. This is quite interesting since the initial Au seed layer thickness had been 3 nm. Hence, it seems that the YBCO density has been altered. On the one hand one could assume this to be due to an incorporation of gold atoms into the YBCO crystal structure. This could be likely because the gold nanoparticles are not only located at the top of the YBCO film as can be seen in figure 1 but also within the YBCO layer itself, i.e. they efficiently distribute over the whole YBCO layer.

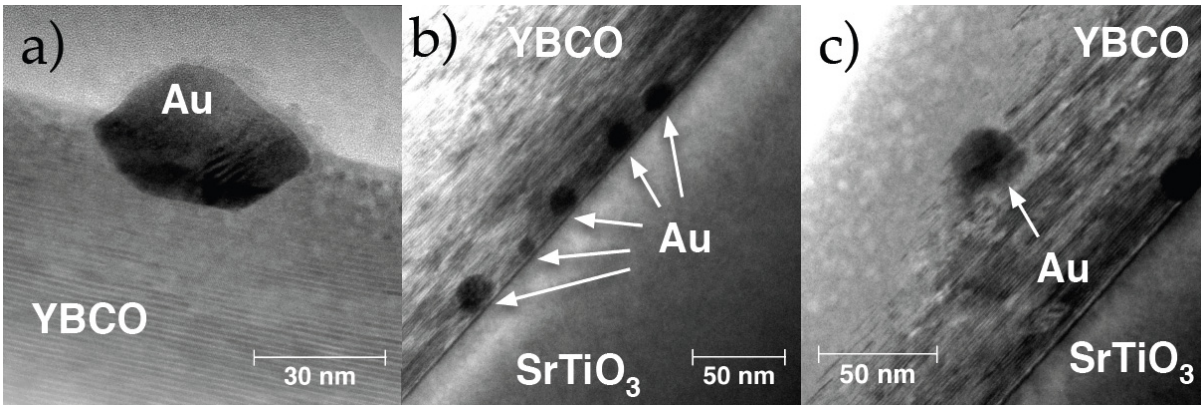

Figure 3. TEM images of crystalline Au nanoparticles: (a) on top of the YBCO layer, (b) at the $SrTiO_3$/YBCO interface and (c) within the YBCO thin film. Reproduced with permission from [20].

This can especially be seen in figure 3 where nanoparticles can be found at the substrate/YBCO interface, on top of the YBCO thin film and also within the YBCO layer itself [20]. Thereby it is noteworthy that the surface of the Au nanoparticles often seems to be faceted, indicating a high crystalline order. Furthermore, it has been shown that Au has a certain solubility in YBCO so one could expect an efficient incorporation of gold atoms [35]. However, an incorporation of gold atoms should lead to an enhancement of the *c*-axis rather than to a thickness reduction as observed by the authors [36]. Furthermore, Rutherford backscattering spectrometry measurements proved that no gold atoms can be found at interstitial places.

On the other hand, our findings could be explained by a variation of the oxygen content $7–\delta$ which determines the length of the YBCO *c*-axis [37]. However, a thickness reduction of 0.6 nm at a YBCO film thickness of 50 nm could only be explained by an extreme variation of the oxygen content from about 6.2 in the non-modified areas to about 6.95 in the area with Au nanoparticles. This would have a severe influence on the superconducting properties such as the critical temperature. Since we did not observe any variation of the critical temperature we do not expect the oxygen content to have caused the observed height variations.

Instead we propose that our findings could be explained by a change in the growth conditions induced by the Au particles. This is also indicated by figure 1 since the surface morphology has been changed in the Au modified areas. Furthermore, x-ray diffraction investigations showed a distinct reduction of macroscopic strain in Au modified regions. If one assumes a reduced number of defects such as dislocations one could also expect the YBCO film thickness to decrease. A more detailed analysis of this question, including high resolution transmission electron microscopy measurements will be part of our future work.

2.3. Magneto-optical results

To show that the incorporation of gold nanoparticles into the YBCO films results in an enhanced critical current density we used spatially resolved magneto-optical measurements. A local and quantitative map of the critical current density across the superconducting thin film can be obtained by magneto-optical microscopy. The setup contains a polarization microscope with a high sensitive CMOS camera and a continuous LHe flow cryostat. On the cooling finger the sample is covered by a Faraday active iron garnet film with a mirror underneath. When the

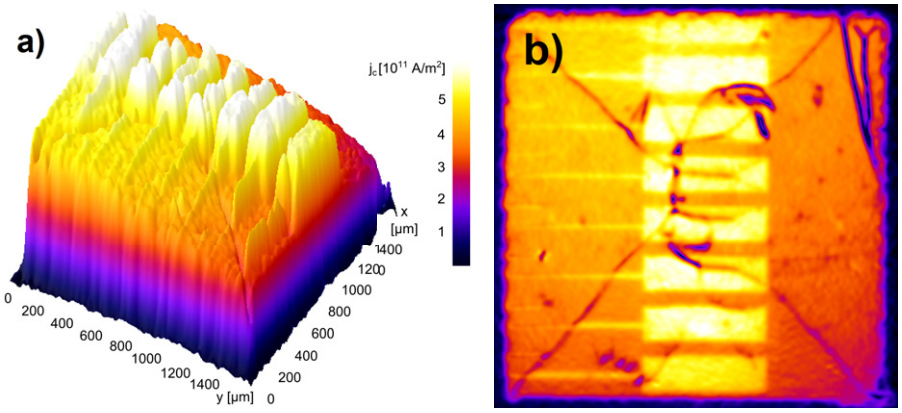

Figure 4. Magneto-optical images obtained at $T = 10$ K: (a) three dimensional colour scale representation of the critical current distribution in an YBCO thin film which was partly modified by embedding Au nanoparticles. (b) Same area as a top view. The critical current density distribution exactly matches the structure pattern of the Au nanoparticles whereby the Au modified areas are characterized by an enhanced critical current density. The dark lines in figure 4(b) are the discontinuity lines where the critical current is bending [39].

iron garnet film is illuminated with linear polarized light, the polarization axis of the light is rotated as a function of the local magnetic field. The degree of rotation is measured by an analyser rotated 90° towards the polarizer. The obtained intensity of the reflected light can be converted into the flux density by a calibration measurement above the critical temperature of the superconductor. A numerical inversion scheme of Biot–Savarts law then provides the local and quantitative map of the critical current density [38].

Figure 4(a) depicts a three dimensional colour scale representation of the critical current distribution in an YBCO thin film in which Au particles were embedded in a distinct pattern. The same part of the sample is shown in figure 4(b) as a top view. The image was obtained in the remnant state: after zero field cooling to $T = 10$ K an external magnetic field of $\mu_0 H = 200$ mT was applied and subsequently removed. As can be seen by comparing the image to the sketch in figure 2, the critical current density distribution exactly matches the structure pattern of the Au nanoparticles. The areas modified with Au are characterized by a higher current density than the areas without Au nanoparticles. At $T = 10$ K the current density can be increased from 4.0×10^{11} to 6.0×10^{11} A m^{-2} by embedding Au nanoparticles. The dark lines in figure 4(b)—also seen as gaps in figure 4(a)—are the discontinuity lines where the critical current is bending [39]. The fact that the critical current density exhibits a finite jump when entering the gold modified regions leads to a number of additional discontinuity lines inside the high current density regions [38]. Under closer inspection of figure 4(b) this additional discontinuity lines can be seen as dark lines in the centre region of panel (b). The geometry of these additional lines is a model independent proof for the enhancement of j_c.

Not only can the modulus of the critical current density be obtained locally from quantitative magneto-optical imaging, but also the hindering of flux line motion can be seen directly when performing magneto-optical imaging in an increasing applied field. The results are depicted in figure 5 where the magnetic flux density inside the partially modified film can

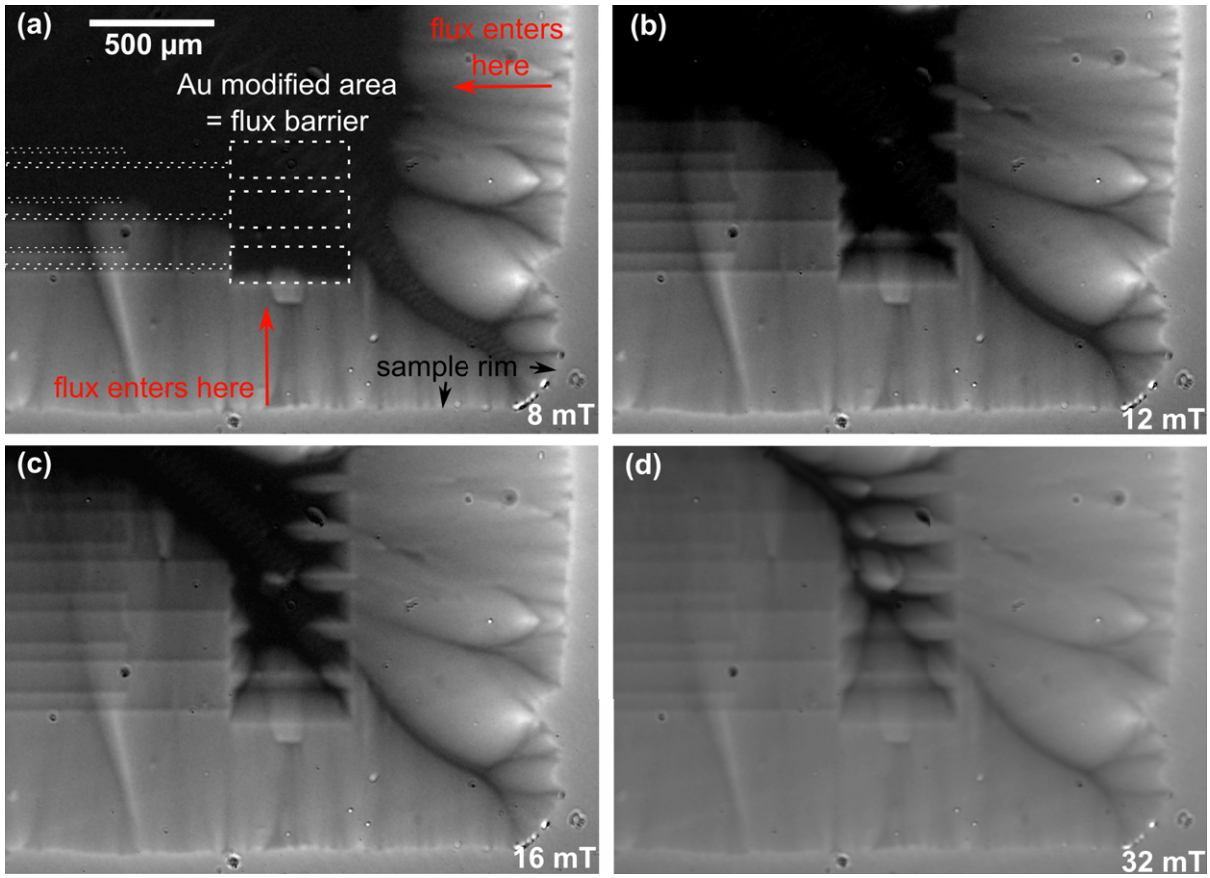

Figure 5. Magneto-optical images of the flux density distribution at $T = 10\,\mathrm{K}$ after zero field cooling in increasing external magnetic field: (a) 8 mT, (b) 12 mT, (c) 16 mT and (d) 32 mT. The rectangular-shaped regions in the centre of the image refer to the parts with nanoparticles.

be seen when gradually increasing the external magnetic field. Bright parts refer to a high local flux density, black parts correspond to $B = 0$.

In all four panels of figure 5 those parts of the YBCO thin film containing Au nanoparticles are located in the centre of the image as sketched in (a). The spatial distribution of the flux density in increasing applied field shows that flux penetration is hindered at the border to these parts. Penetration within the Au modified parts takes place at higher external fields than in the pristine parts. At the border, where the flux motion is hindered the flux density increases which can be seen as brighter lines in the images.

In summary, the magneto-optical images of the flux density show a hindering of the flux line motion in the Au modified areas. The critical current density in the remnant state is enhanced in the same areas. Since flux density motion and critical current density are mutually dependent these two phenomena have the same reason: an enhanced pinning in these areas. Owing to the fact that the Au modified areas do not show an additional formation of precipitates, one can expect that an enhanced critical current density in the Au modified areas can only result from an additional pinning of flux lines induced by the Au nanoparticles.

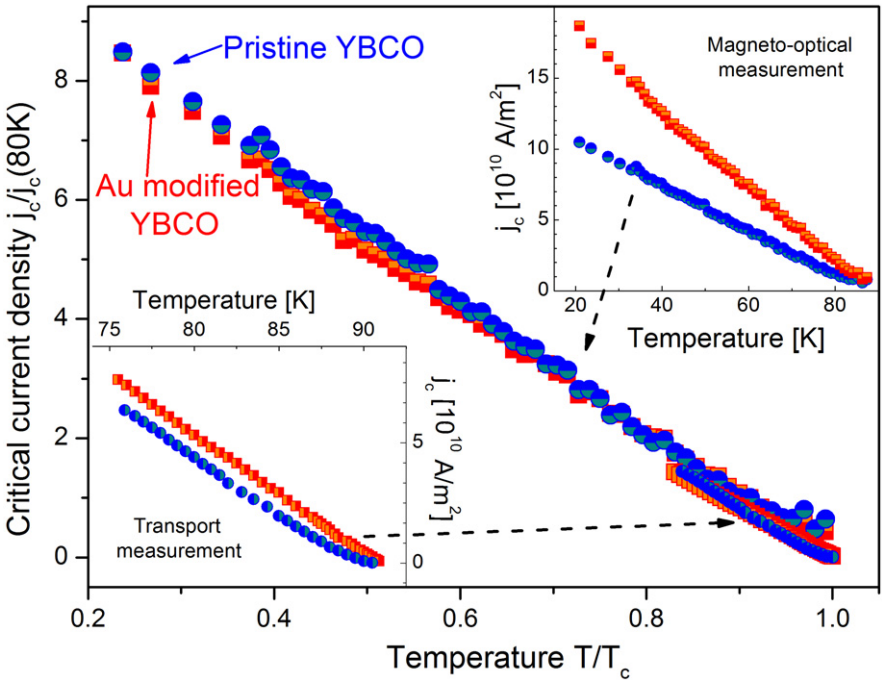

Figure 6. Normalized temperature dependence of the local critical current density obtained by transport measurements as well as by magneto-optical measurements. Both methods allow measuring of the two different areas separately. Note that the curve progression remains the same with and without the Au nanoparticles.

2.4. Temperature dependence of the critical current density

We now want to address the question of the origin of this additional pinning. Two scenarios are possible: firstly, vortices can be directly pinned at the gold nanoparticles. Secondly, the presence of the nanoparticles can induce a structural change of the superconductor during growth which then leads to an 'improved YBCO' as described before for the case of BZO doped YBCO [25]. Our method of distinguishing between the two possible mechanisms is to look at the temperature dependence of the local critical current density, which can be regarded as a fingerprint of different pinning scenarios [29].

In our case, the investigations have to be performed locally to avoid an averaging of modified and pristine areas. The relevant data obtained from film parts with and without nanoparticles, respectively, is again provided by magneto-optical measurements. In order to give an additional proof for the high accuracy of the method used, additional transport measurements have been performed on different samples. All results are presented in figure 6.

As can be seen, the temperature dependence obtained from transport measurements and magneto-optical imaging reveals the same curve progression for both the pristine YBCO and the Au modified YBCO. The difference in the absolute values measured with both methods can be explained by the fact that different samples were measured. In doing so, all of the samples investigated showed an enhancement of the critical current density in the Au modified areas. A possible correlation between the current density enhancement and the initial Au seed layer thickness, and thus cluster size and distribution, will be part of our future research. All

data obtained proved that the temperature dependence of the critical current density remains unchanged when Au particles were embedded. Since the shape of the temperature dependence is a direct indication of the pinning scenario, it can be concluded that flux pinning at individual Au nanoparticles only plays a minor role. Otherwise, the shape of the $j_c(T)$ curves would change more significantly [29]. By considering the volume of the initial Au seed layer and assuming no desorption of Au atoms during the heating process (which is rather conservative) one calculates the gold volume to be below 6% of the final film's volume. Although also this volume can be accounted for by a pinning of flux vortices, the contribution appears to be rather small. Interestingly, it can be noted that both $j_c(T)$ curves show an almost linear temperature dependence. This indicates that there is nearly no suppression of the current flow by low-angle grain boundaries which would lead to a much more pronounced drop of j_c with increasing temperature [27, 29]. Since this behaviour is not only found in the Au modified but also in the pristine areas of the YBCO thin film, we suggest that our growth conditions during the PLD process reduce the number of low-angle grain boundaries. In conclusion, by considering the $j_c(T)$ curves, we can state that the presence of Au nanoparticles mainly increases the pinning force density which is already generated by the YBCO structure itself. This clearly supports the model that the inclusion of nanoparticles as APCs in YBCO reaches its goal via a modification of the YBCO structure. The contribution of direct pinning at the nanoparticles themselves is rather small.

Since a strain distribution has to be inhomogeneous on very short length scales for an effective pinning we can now conclude that the spatially controlled inclusion of Au nanoparticles into YBCO films can be realized with high accuracy. The limiting factor of the spatial resolution of our artificial pinning landscapes is given by the lithography process that is used to pattern the very thin gold layers. In our case this would be of the order of one micrometre, a possible electron beam lithography process would probably be able to enhance this performance to even smaller structures.

3. Conclusions

We have generated controlled flux pinning patterns in strong pinning YBCO thin films by spatially resolved inclusion of Au nanoparticles. Thereby we managed to enhance the critical current density from 4.0×10^{11} to $6.0 \times 10^{11}\,\mathrm{A\,m^{-2}}$ at $T = 10\,\mathrm{K}$ in the gold modified areas. Comparing the temperature dependence of the critical current density we showed that pinning is realized by a gold induced modification of the YBCO structure and not by an additional pinning at individual gold particles. This allows the production of smart YBCO films with tailored patterns of the critical current density. Arbitrary flux pinning structures can be generated in thin YBCO films that can be used as ideal templates for the production of advanced superconducting structures such as magnetic sensors or electronic devices.

Acknowledgments

CK thanks the Landesgraduiertenförderung Thüringen for financial support. Furthermore, we thank J Dellith from the Institute of Photonic Technology (IPHT) for technical support. The authors are also grateful to the members of the Scientific Service Group Technology of the Max Planck Institute for Solid State Research for etching the sample.

References

[1] Koelle D, Kleiner R, Ludwig F, Dantsker E and Clarke J 1999 High-transition-temperature superconducting quantum interference devices *Rev. Mod. Phys.* **71** 631

[2] Makhlin Y, Schon G and Shnirman A 2001 Quantum-state engineering with Josephson-junction devices *Rev. Mod. Phys.* **73** 357

[3] Wunderlich S, Redlich L, Schmidl F, Dörrer L, Köhler T and Seidel P 2000 Inductance matching of high-T_C dc-SQUIDs in planar gradiometers using a laser patterning technique *Physica* C **340** 51

[4] Marx A and Gross R 1997 Scaling behavior of $1/f$ noise in high-temperature superconductor Josephson junctions *Appl. Phys. Lett.* **70** 120

[5] Dantsker E, Tanaka S and Clarke J 1997 High-T_c super conducting quantum interference devices with slots or holes: low $1/f$ noise in ambient magnetic fields *Appl. Phys. Lett.* **70** 2037

[6] Matsumoto K and Mele P 2010 Artificial pinning center technology to enhance vortex pinning in YBCO coated conductors *Supercond. Sci. Technol.* **23** 014001

[7] Foltyn S R, Civale L, Macmanus-Driscoll J L, Jia Q X, Maiorov B, Wang H and Maley M 2007 Materials science challenges for high-temperature superconducting wire *Nature Mater.* **6** 631

[8] Dam B *et al* 1999 Origin of high critical currents in $YBa_2Cu_3O_{7-\delta}$ superconducting thin films *Nature* **399** 439

[9] Klaassen F C, Doornbos G, Hujibregtse J M, van der Geest R C F, Dam B and Griessen R 2001 Vortex pinning by natural linear defects in thin films of $YBa_2Cu_3O_{7-\delta}$ *Phys. Rev.* B **64** 184523

[10] Schuster T, Kuhn H, Koblischka M R, Theuss H, Kronmüller H, Leghissa M, Kraus M and Saemann-Ischenko G 1993 Enhancement of critical current densities by heavy-ion irradiation in $YBa_2Cu_3O_{7-\delta}$ observed using the high-resolution Faraday effect *Phys. Rev.* B **47** 373

[11] Raveau B, Michel C, Hervieu M, Groult D, Maignan A and Provost J 1992 How to optimize high-T_c superconductive cuprates *J. Supercond.* **5** 203

[12] Albrecht J, Leonhardt S and Kronmüller H 2001 Influence of vortex–vortex interaction on critical currents across low-angle grain boundaries in $YBa_2Cu_3O_{7-\delta}$ thin films *Phys. Rev.* B **63** 014507

[13] Maiorov B, Baily S A, Zhou H, Ugurlu O, Kennison J A, Dowden P C, Holesinger T G, Foltyn S R and Civale L 2009 Synergetic combination of different types of defect to optimize pinning landscape using $BaZrO_3$-doped $YBa_2Cu_3O_7$ *Nature Mater.* **8** 398

[14] Berdiyorov G R, Milosevic M V and Peeters F M 2009 Composite vortex ordering in superconducting films with arrays of blind holes *New J. Phys.* **11** 013025

[15] Jooss C, Warthmann R and Kronmüller H 2000 Pinning mechanism of vortices at antiphase boundaries in $YBa_2Cu_3O_{7-\delta}$ *Phys. Rev.* B **61** 12433

[16] Djupmyr M, Christiani G, Habermeier H U and Albrecht J 2005 Anisotropic temperature-dependent current densities in vicinal $YBa_2Cu_3O_{7-\delta}$ *Phys. Rev.* B **72** 220507

[17] Martinez B, Obradors X, Gou A, Gomis V, Pinol S, Fontcuberta J and VanTol H 1996 Critical currents and pinning mechanisms in directionally solidified $YBa_2Cu_3O_7 - Y_2BaCuO_5$ composites *Phys. Rev.* B **53** 2797

[18] Haugan T, Barnes P N, Wheeler R, Meisenkothen F and Sumption M 2004 Addition of nanoparticle dispersions to enhance flux pinning of the $YBa_2Cu_3O_{7-x}$ superconductor *Nature* **430** 867

[19] MacManus-Driscoll J L, Harrington S A, Durrell J H, Ercolano G, Wang H, Lee J H, Tsai C F, Maiorov B, Kursomovic A and Wimbush S C 2010 High current, low cost YBCO conductors—what's next? *Supercond. Sci. Technol.* **23** 034009

[20] Katzer C *et al* 2011 Increased flux pinning in $YBa_2Cu_3O_{7-\delta}$ thin-film devices through embedding of Au nano crystals *Europhys. Lett.* **95** 68005

[21] MacManus-Driscoll J L, Foltyn S R, Jia Q X, Wang H, Serquis A, Civale L, Maiorov B, Hawley M E, Maley M P and Peterson D E 2004 Strongly enhanced current densities in superconducting coated conductors of $YBa_2Cu_3O_{7-x} + BaZrO_3$ *Nature Mater.* **3** 439

[22] Peurla M, Paturi P, Stepanov Y P, Huhtinen H, Tse Y Y, Boodi A C, Raittila J and Laiho R 2006 Optimization of the $BaZrO_3$ concentration in YBCO films prepared by pulsed laser deposition *Supercond. Sci. Technol.* **19** 767

[23] Gutierrez J *et al* 2007 Strong isotropic flux pinning in solution-derived $YBa_2Cu_3O_{7-x}$ nanocomposite superconductor films *Nature Mater.* **6** 367
[24] Holesinger T G *et al* 2008 Progress in nanoengineered microstructures for tunable high-current, high-temperature superconducting wires *Adv. Mater.* **20** 391
[25] Llordés A *et al* 2012 Nanoscale strain-induced pair suppression as a vortex-pinning mechanism in high-temperature superconductors *Nature Mater.* **11** 329
[26] Laviano F, Gerbaldo R, Ghigo G, Gozzelino L, Minetti B and Mezzetti E 2011 Study and application of controlled vortex dynamics in patterned YBCO films *J. Supercond. Nov. Magn.* **24** 75
[27] Brück S and Albrecht J 2005 Experimental evidence of the dominant role of low-angle grain boundaries for the critical current density in epitaxially grown $YBa_2Cu_3O_{7-\delta}$ thin films *Phys. Rev.* B **71** 174508
[28] Albrecht J, Leonhardt S, Habermeier H U, Brück S, Spolenak R and Kronmüller H 2004 Enhanced flux line pinning by substrate induced defects in YBCO thin films *Physica* C **404** 18
[29] Albrecht J, Djupmyr M and Brück S 2007 Universal temperature scaling of flux line pinning in high-temperature superconducting thin films *J. Phys.: Condens. Matter* **19** 216211
[30] Wollman D A, VanHarlingen D J, Lee W C, Ginsberg D M and Leggett A J 1993 Experimental determination of the superconducting pairing state in YBCO from the phase coherence of YBCO-Pb dc SQUIDs *Phys. Rev. Lett.* **71** 2134
[31] Grosse V, Engmann S, Schmidl F, Undisz A, Rettenmayr M and Seidel P 2010 Formation of gold nanoparticles during pulsed laser deposition of $YBa_2Cu_3O_{7-\delta}$ thin films *Phys. Status Solidi (RRL)* **4** 97
[32] Michalowski P, Schmidt M, Schmidl F, Grosse V, Kuhwald D, Katzer C, Hübner U and Seidel P 2011 Engineering of $YBa_2Cu_3O_{7-\delta}$ grain boundary Josephson junctions by Au nanocrystals *Phys. Status Solidi (RRL)* **5** 268
[33] Zakosarenko V, Schmidl F, Schneidewind H, Dörrer L and Seidel P 1994 Thin-film dc SQUID gradiometer using a single $YBa_2Cu_3O_{7-x}$ layer *Appl. Phys. Lett.* **65** 779
[34] Mannhart J, Bednorz J G, Catana A, Gerber C and Schlom D G 1994 *Materials and Crystallographic Aspects of HTC-Superconductivity* ed E Kaldis (Dordrecht: Kluwer) pp 453–70
[35] Bohnenkamp-Weiss R and Schmid-Fetzer R 1994 Chemical stability at noble metal M/$YBa_2Cu_3O_{6.8}$ interfaces (M = Pt, Ag, Au). *Physica* C **220** 396
[36] Nguyen van Huong C, Nicolas M, Dubon A and Hinnen C 1993 Superconducting properties of $YBa_2Cu_3O_7$-Au composites *J. Mater. Sci.* **28** 6418
[37] Benzi P, Bottizzo E and Rizzi N 2004 Oxygen determination from cell dimensions in YBCO superconductors *J. Cryst. Growth* **269** 625
[38] Jooss C, Albrecht J, Leonhardt S, Kuhn H and Kronmüller H 2002 Magneto-optical studies of current distributions in high-T_c superconductors *Rep. Prog. Phys.* **65** 651
[39] Schuster T, Indenbom M V, Koblischka M R, Kuhn H and Kronmüller H 1994 Observation of current-discontinuity lines in type-II superconductors *Phys. Rev.* B **49** 3443